ARTICLE

Sustained Release of Doxorubicin through Semi-Interpenetrating Polymer Network-Stabilized Micelles

Juyoung Hwang[1,2,3] · Min-Hee Jo[3] · Chen Li[4] · Sun Joo Park[3] · Minseok Kwak[1,2,3,5]

Abstract

Developing effective drug delivery systems plays an important role in improving the therapeutic outcomes of anticancer agents. In this study, we investigated the potential of a micellar delivery system modified with semi-interpenetrating polymer networks (sIPN) to enhance the therapeutic efficacy of doxorubicin (Dox), a widely used chemotherapeutic agent. The sIPN-modified micelles were prepared by loading polymerizable tetraacrylate moiety into the core of sodium dodecyl benzene sulfonate (SDBS) micelles. To evaluate the stability of SDBS-micelle and SDBS-sIPN, we assessed the stability of the micellar structure under critical micelle temperature conditions. The results demonstrated that incorporating sIPN significantly enhanced the structural stability of the micelles, particularly in response to acrylate unit concentrations, leading to the 60 days continuous release of Dox. Furthermore, we examined the ability of SDBS-micelle-Dox and SDBS-sIPN-Dox to induce apoptosis and necrosis in HeLa cells. Annexin V/PI double staining and flow cytometry analysis revealed that SDBS-sIPN-Dox exhibited a sustained release profile of Dox, resulting in a reduced apoptotic response compared to free Dox and SDBS-micelle-Dox in the given time. These findings highlight the potential of the sIPN-modified micellar delivery system as an efficient drug delivery platform, enabling sustained release and minimizing adverse side effects associated with immediate drug release. The sustained release profile achieved through incorporation of sIPN structures holds great promise for improving the therapeutic outcomes of anticancer agents.

Graphical Abstract

Extended author information available on the last page of the article
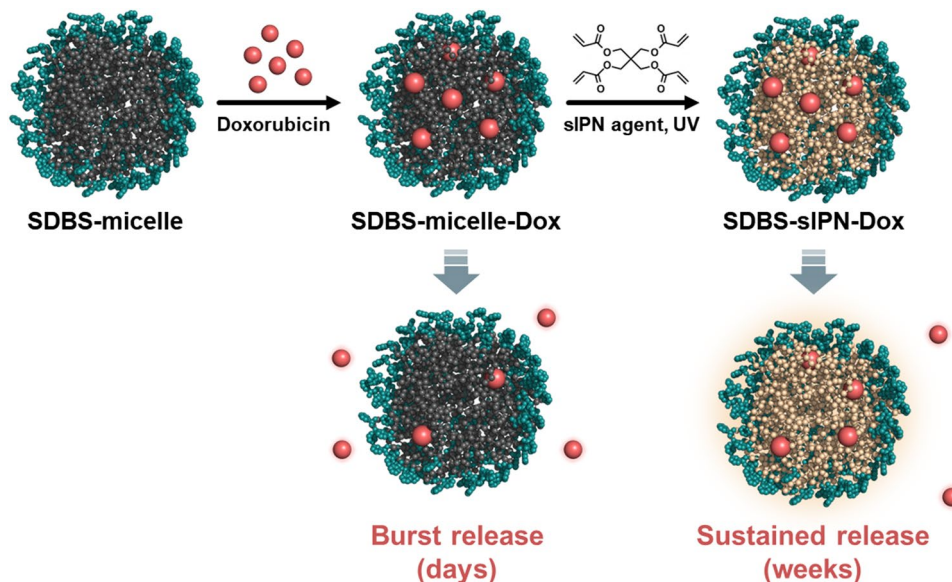
This study involved the fabrication of semi-interpenetrating polymer network (sIPN)-stabilized micelles using an FDA-approved surfactant and loading anti-cancer drug inside. The stability of the resulting stabilized micelle and the prolonged release of the drug, doxorubicin, were evaluated. The findings underscore the potential of sIPN-stabilized micelles as an effective drug delivery platform, capable of providing sustained release and improving therapeutic outcomes for anticancer drugs.

1 Introduction

Chemotherapy is a widely used therapeutic approach for various types of cancer to eliminate cancer cells or inhibit their growth [1]. The effectiveness of cancer chemotherapy is often limited by its toxicity to healthy tissues [2]. This limitation arises from two factors: the non-specificity of anticancer agents towards cancerous tissues and the poor biopharmaceutical properties of the drug [3]. However, with the advancements in chemotherapy technology, there is a growing trend to use anticancer compounds characterized by higher molecular weight and lower aqueous solubility [4]. While these properties synergistically contribute to enhanced drug-receptor binding, they concurrently pose challenges regarding drug solubility and membrane permeability [5].

Most anticancer agents are administered intravenously, resulting in an initial burst release of the drug followed by a rapid decrease in drug concentrations below effective therapeutic levels in the bloodstream [6]. Controlled release formulations have demonstrated that prolonged exposure of affected tissues to moderate drug concentrations is more advantageous than intermittent high-concentration drug delivery [7, 8]. The limitations associated with conventional anticancer drug formulations have prompted extensive efforts to develop more effective chemotherapy formulations.

One of the commonly employed chemotherapeutic agents is doxorubicin (Dox), a potent anthracycline antibiotic known for its effectiveness against a wide range of malignancies [9, 10]. Doxorubicin functions by intercalating with DNA, preventing DNA replication and transcription, and inducing cell death [11, 12]. However, its therapeutic efficacy is hampered by dose-dependent cardiotoxicity, myelosuppression, and the development of multidrug resistance [13–15]. These adverse effects associated with conventional Dox formulations have spurred researchers to explore alternative approaches, such as prodrug strategies or encapsulation of Dox in particulate carriers [16–19]. One promising process involves the association of Dox with nanoparticulate carriers, including hydrogels, liposomes, or micelles [20–22]. These nano-sized vehicles enable the controlled release of Dox over extended periods, thereby increasing its efficacy and reducing toxic side effects. [23–25]

Due to the self-assembly of surfactants, micelles can readily disassemble below their critical micelle temperature (CMT) and/or critical micelle concentration (CMC) [26, 27]. In this study, we demonstrate the successful dispersion of poorly water-soluble Dox through the utilization of a water-soluble micelle system based on FDA-approved sodium dodecylbenzene sulfonate (SDBS). SDBS surfactants spontaneously form nano-sized micelles with a hydrophobic core and hydrophilic shell via micro-phase separation in aqueous media [28–30]. Additionally, to enhance the stability of the SDBS-micelle below its CMT and CMC, we have implemented a semi-interpenetrating polymer network (sIPN) system [31, 32]. This approach involves the formation of a network structure within the micelle core by subjecting it to ultraviolet (UV) irradiation in the presence of a crosslinking agent. The crosslinking agent employed is pentaerythritol tetraacrylate (PETA), which undergoes intermolecular crosslinking via radical polymerization initiated by UV irradiation [33]. Therefore, a mesh-like formation within the micelle core, namely SDBS-sIPN, allows for the enhancement of physical properties without chemical modifications to the surfactant chain.

sIPN-modified micelles offer distinct advantages over hydrogels and liposomes in drug delivery. Hydrogels have been widely employed for localized drug delivery, enabling controlled release to specific tissues or organs at the targeted delivery site [34–38]. Liposomes have a limited loading capacity to encapsulate hydrophobic drugs and often suffer from drug leakage during storage and circulation, leading to decreased drug stability and efficacy. [39, 40]

In contrast, sIPN micelles overcome these challenges by serving as an efficient drug encapsulation platform. The hydrophobic core of sIPN micelles enables high drug loading, enhancing stability even at low concentrations and temperatures and mitigating the potential for drug leakage and degradation [33]. These inherent advantages position sIPN micelles as a promising alternative to hydrogels and liposomes, particularly for applications that demand systemic and sustained drug release.

In this study, we adapted the micelle stabilization using the sIPN approach and subsequently investigated the stability of SDBS-sIPN-Dox in an aqueous environment. Additionally, we evaluated the ability of the sustained release of Dox from both the SDBS-micelle and SDBS-sIPN. Furthermore, we investigated the cytotoxicity in HeLa cell induced by Dox in these systems.

2 Experimental

2.1 SDBS-micelle and SDBS-sIPN formation

The SDBS-micelle and SDBS-sIPN were synthesized according to the procedure outlined in our published reports [33]. First, 0.5 g SDBS (TCI, Japan) was dissolved in chloroform (Daejeong, Korea) in one glass vial. Simultaneously, different amounts of PETA (Sigma-Aldrich, MO, USA) were added to separate glass vials at weight ratios of 0%, 0.5%, 1%, and 2% relative to the SDBS. The organic solvents were then evaporated completely using a rotary evaporator, resulting in SDBS and PETA films. Next, the SDBS film was hydrated by adding 4.5 mL of an aqueous Dox solution (Santa Cruz, CA, USA) to the vial, and the mixture was stirred at r.t. using a shaker at 200 rpm for 12 h. Subsequently, the SDBS-Dox solution was transferred to the PETA-filmed vial and stirred for another 12 h. The vial was purged with argon gas and heated at 60 °C for 10 min. Then, a cover glass was placed over the vial, and the mixture was exposed to UV radiation from a Lumen Dynamic Omnicure series 200 UV lamp with a 320—500 nm filter at a power of 1.5 W/cm^2 at 50 °C for 6 min to crosslink the SDBS-Dox micelle core with PETA. Finally, the SDBS-sIPN was obtained by slowly cooling down the UV-exposed solution to a temperature of 25 °C. Any remaining PETA and Dox residues were removed by passing the solution through a 0.2 μm Minister® syringe filter (Sartorius Stedim, France).

2.2 CMT test

A CMT test was conducted to evaluate the stability of SDBS-micelles and SDBS-sIPN. Each sample, consisting of 0.5 mL of SDBS-micelle and SDBS-sIPN, was refrigerated at 4 °C for 3 h. Subsequently, centrifugation was carried out at a speed of 12,000 rpm and a temperature of 4 °C for 10 min. The absorbance and fluorescence of the supernatant were measured using a SpectraMax M2 spectrophotometer (Molecular Devices, CA, USA) to assess the results of the CMT test. The hydrodynamic diameter of SDBS-micelle and SDBS-sIPN was evaluated using a Zetasizer Nano ZS device (Malvern Instruments, Worcestershire, UK) that was equipped with a 4.0 mV He–Ne laser (633 nm).

2.3 Dox release test

Both the SDBS-micelle and SDBS-sIPN samples were subjected to centrifugation at a speed of 12,000 rpm for 60 min at a temperature of 20 °C on the designated days. Subsequently, the absorbance and fluorescence of the supernatant were measured.

2.4 Cell line

The human cervical cancer HeLa cells were purchased from the American Type Culture Collection (ATCC, VA, USA) and maintained in Dulbecco's modified Eagle medium (Welgene, Republic of Korea) supplemented with 10% fetal bovine serum (Welgene, Republic of Korea), 100 U/mL of penicillin, and 100 μg/mL of streptomycin. The cells were cultured in a CO_2 incubator at 37 °C with 5% CO_2.

2.5 MTT assay for cytotoxicity evaluation

The 3-(4,5-dimethylthiazol-2-yl)-2,5-diphenyltetrazolium bromide (MTT) assay was conducted to evaluate the cytotoxicity of SDBS-micelle and SDBS-sIPN. HeLa cells were plated at a density of 6×10^3 cells per well in 96-well plates. After 24 h of incubation, the cells were exposed to phosphate-buffered saline (PBS), SDBS-micelle, or SDBS-sIPN for 24 h or 48 h. Subsequently, the cells were treated with an MTT solution at a final 1 mg/mL concentration and incubated for 4 h at 37 °C. The formazan crystals obtained were solubilized in 100 μL of dimethyl sulfoxide (DMSO), and the absorbance was recorded at a wavelength of 595 nm using a microplate reader (FilterMax F5, Molecular Devices).

2.6 Apoptosis assay

The HeLa cells were plated in a 12-well plate at a density of 6.9×10^4 cells/well. After 24 h of incubation, the cells were treated with either PBS, SDBS-micelle, SDBS-sIPN, SDBS-micelle-Dox, or SDBS-sIPN-Dox for 48 h. Following treatment, the cells were washed with PBS, resuspended in 100 μL of the solution, and stained with Annexin V-FITC and PI using the FITC Annexin V Apoptosis Detection Kit from BD Biosciences (CA, USA). The stained cells were incubated in a light-protected environment at a temperature of 24 °C for 10 min. Subsequently, the samples were analyzed using a FACSVerse™ flow cytometer from BD Bioscience. The fluorescence signals were detected at excitation and

emission wavelengths of 488 nm and 530 nm, respectively. The acquired data were analyzed using flowJo™ Software from BD Bioscience.

2.7 Statistical analysis

The data are presented as the mean ± standard deviation of the mean. One-way analysis of variance (ANOVA) was used to analyze the p-value, with statistical significance set at $**p < 0.01$.

3 Results and discussion

3.1 Characterization of SDBS-sIPN formulation

The formation of micelles in SDBS is known to be sensitive to temperature changes, and the temperature at which micellization occurs is referred to as the CMT. Below the CMT, SDBS micelles undergo dissociation into individual unimers, resulting in the release of molecules encapsulated within the micelle core. To investigate the potential of incorporating sIPN within the SDBS micelle to enhance the stability of the core–shell structure and the encapsulation efficiency of Dox at temperatures below its CMT (4 °C). To evaluate the effect of PETA on sIPN formation, samples with varying contents of PETA ranging from 0 to 2% relative to the fixed weight of SDBS were prepared, and the absorbance and fluorescence spectra of Dox were analyzed. Figure 1a and Figures S1 revealed that the extent of sIPN formation was significantly influenced by the PETA content, with higher PETA concentrations promoting the formation of stable sIPNs.

Furthermore, increasing the PETA content up to 1% resulted in enhanced Dox loading capacity, while 1% and 2% exhibited comparable optical properties. Conversely, micelles containing lower PETA (below 1.0%) exhibited decreased absorption intensity at temperatures below the

CMT, suggesting suboptimal network formation within the micelle core. The hydrodynamic diameters of SDBS-micelle and SDBS-sIPN were determined using DLS to assess the influence of PETA content on the stability of the micellar structure under the CMT. Figure 1b demonstrated an increase in hydrodynamic diameter for SDBS-sIPN containing 1% and 2% PETA, indicating swelling or expansion of the micellar structure. However, SDBS-micelle (PETA 0%) and SDBS-sIPN (PETA 1%) showed minimal changes in diameter after the CMT test, indicating the absence or weaker presence of sIPN structures. Thus, we determined that an optimal PETA content of 1% facilitated the formation of robust sIPNs, which exhibited excellent stability (99.2% retained absorption, 99.6% retained fluorescence) and high Dox loading capacity.

3.2 Sustained Dox release by sIPN structure

SDBS-sIPN formulations containing 1% PETA, determined as the optimal PETA content, were synthesized, and their absorbance and fluorescence spectra were analyzed. The absorption spectrum exhibited a peak wavelength of 500 nm, while fluorescence peaks were observed at 550 and 590 nm when excited at 470 nm (Fig. 2). To assess the release profile of Dox from SDBS-micelle-Dox and SDBS-sIPN-Dox in
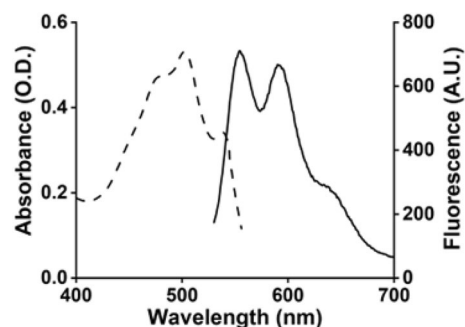
Fig. 2 Absorption and fluorescent spectra of Doxorubicin into SDBS-sIPN (SDBS-sIPN-Dox). λ_{ex}: 470 nm
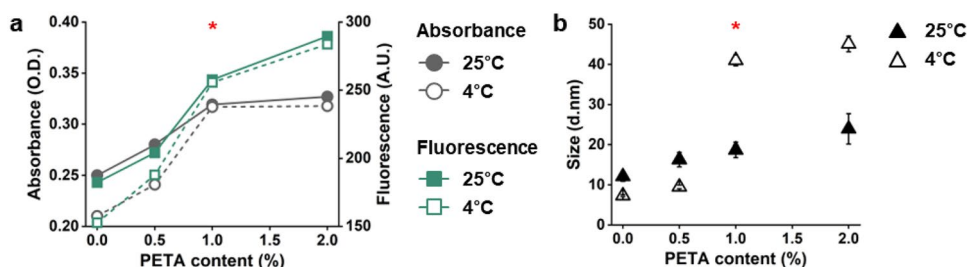
Fig. 1 Optical properties of SDBS-micelle and SDBS-sIPN. **a** Absorption and fluorescent values of Dox loaded with SDBS-micelle (without PETA) and SDBS-sIPN at different PETA contents. λ_{abs}: 500 nm, λ_{ex}: 470 nm, λ_{em}: 550 nm. **b** The hydrodynamic sizes of

SDBS-micelle and SDBS-sIPN with varying PETA contents were measured using dynamic light scattering. The asterisks presented in the figure indicate the concentration of PETA utilized for the preparation of SDBS-sIPN in this study

Fig. 3 Decrease in absorption and fluorescence intensity of Doxorubicin into SDBS-micelle and SDBS-sIPN. λ_{abs}: 500 nm, λ_{ex}: 470 nm, λ_{em}: 590 nm
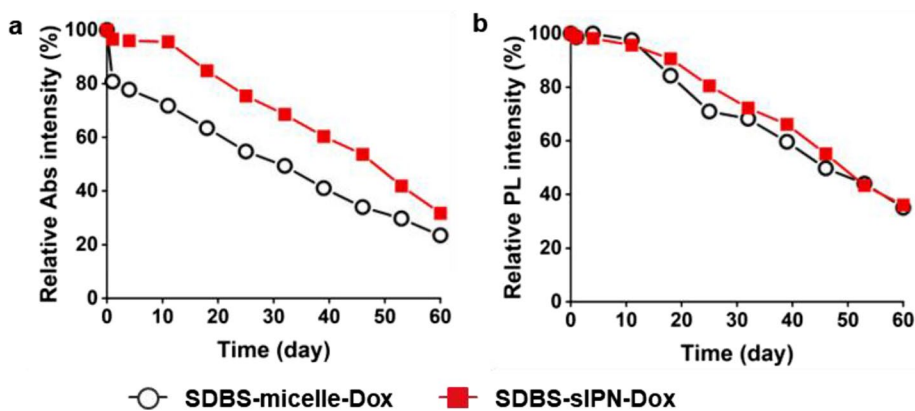

PBS buffer, cumulative Dox were plotted over time (Fig. 3a and b). The release of Dox was determined by monitoring the decrease in intensity using a spectrophotometer at $\lambda_{abs} = 500$ nm and $\lambda_{em} = 590$ nm (Figure S2). The results indicated distinct release patterns for SDBS-micelle-Dox and SDBS-sIPN-Dox formulations. SDBS-micelle-Dox demonstrated an initial burst release (ca. 20%) within the first 2 days, followed by a steady release of approximately 50% of the initially loaded drug over 30 days at r.t. (Fig. 3a and b). These findings indicate the instability of the SDBS-micelle structure below the CMC, leading to the subsequent release of the encapsulated Dox, which might contribute to severe side effects for cancer patients. In contrast, SDBS-sIPN-Dox showed a sustained and prolonged release, extending 20% less release in two weeks. This finding provides that incorporating sIPN into the core of SDBS micelles greatly impacts enhancing the structural stability of the nanoparticles, particularly in response to concentration changes. Thus, the SDBS-sIPN structure enables stable and controlled release of Dox from the nanoparticles.

3.3 Induction of apoptosis and necrosis by SDBS-sIPN-Dox

The cytotoxicity of SDBS-micelle and SDBS-sIPN formulations was evaluated in HeLa cells, a well-established human breast cancer cell line, using the MTT assay. Notably, the results from Figure S3 demonstrated no significant cytotoxic effects for pristine SDBS-micelle and SDBS-sIPN formulations in the absence of Dox. Therefore, SDBS-micelle and SDBS-sIPN suggested these delivery systems' inherent biocompatibility and safety. Based on previous reports, it has been established that soluble Dox is capable of inducing apoptotic and necrotic cell death in various cancer cell lines [41, 42]. Therefore, we examined the potential of SDBS-micelle-Dox and SDBS-sIPN-Dox formulations in inducing apoptosis and necrosis in HeLa cells. Annexin V/PI double staining was employed to assess the cellular response, followed by flow cytometry analysis.

Interestingly, SDBS-sIPN-Dox exhibited a remarkable absence of significant apoptotic and necrotic response after 48 h of treatment, which can be attributed to the sustained release of Dox by the sIPN structure (Fig. 4, Figure S4). In

Fig. 4 Percentage of Annexin V and propidium iodide (PI) stained cell populations in HeLa cells treated with free Dox, SDBS-micelle-Dox, and SDBS-sIPN-Dox at various Dox concentrations after 48 h of incubation. Each bar in the graph indicates the mean
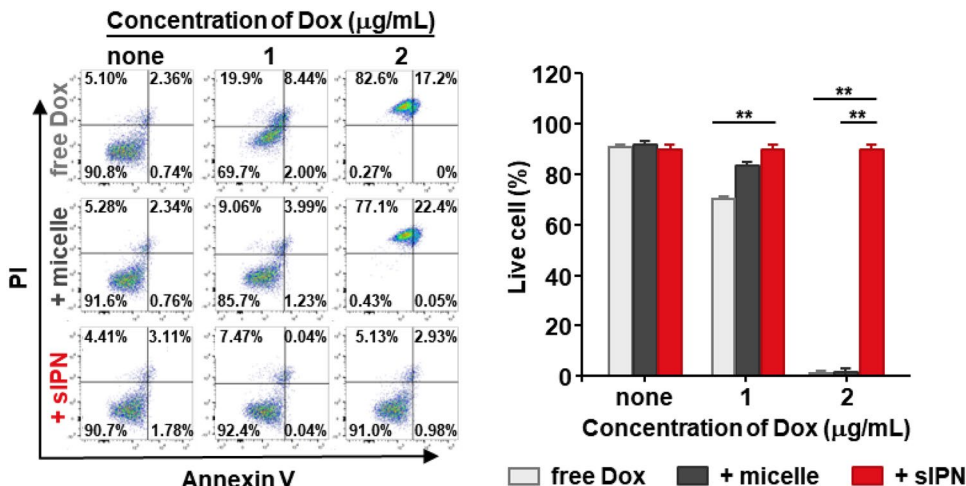
contrast, free Dox and SDBS-micelle-Dox elicited induction of both apoptotic and necrotic cell death, most likely attributable to the rapid release of Dox from these formulations (Fig. 4, Figure S4). These findings underline the crucial role of the sIPN structure in controlling the release profiles of Dox and minimizing adverse side effects associated with its rapid release. Taken together, these findings demonstrate the enormous potential of SDBS-sIPN-Dox as a drug delivery system that effectively minimizes the side effects related to the rapid release of Dox. Incorporating the sIPN structure results in a long-lasting release profile that allows for regulated and targeted delivery of the drug, improving therapeutic effects while reducing cytotoxicity. These findings provide a valuable and promising strategy for developing advanced drug delivery systems for enhanced therapeutic efficacy in cancer treatment.

4 Conclusions

In conclusion, this study demonstrates the successful development of an sIPN-modified micellar delivery system for enhancing the therapeutic efficacy of Dox. Incorporating sIPN into the core of SDBS micelles significantly improved the structural stability of the nanoparticles, allowing for sustained release of Dox. In test tubes, the release rate in two weeks was 20% slower for the stabilized micelle compared to the non-stabilized one. Considering the chemotherapy cycle for drug administration is commonly set to two weeks, this sustained release profile merits potential application in drug delivery of hydrophobic drugs. The evaluation of cytotoxicity using the MTT assay revealed no significant cytotoxic effects of the SDBS-micelle and -sIPN formulations, indicating their biocompatibility. Furthermore, the investigation of apoptotic and necrotic responses in HeLa cells demonstrated that the SDBS-sIPN-Dox exhibited a sustained release profile of Dox, leading to reduced apoptotic and necrotic induction compared to free Dox and SDBS-micelle-Dox in 48 h. These findings highlight the potential of the sIPN-modified micellar delivery system as a promising strategy for improving the therapeutic outcomes of Dox. The sustained release of Dox achieved through the incorporation of sIPN structures offers advantages in minimizing adverse side effects associated with rapid drug release. By providing controlled and prolonged drug release, the sIPN-modified micelles can enhance the efficacy of Dox while reducing its cytotoxic effects. Additionally, the potential of combining this sIPN-modified micellar system with other therapeutic agents should be explored to maximize its

therapeutic potential in vivo for a long time. Overall, the sIPN-modified micellar delivery system represents a practical approach to improving the effectiveness of anticancer drug delivery, providing a foundation for developing more efficient and targeted cancer therapies in the near future.

Declarations

Conflict of interest There are no conflicts to declare.

References

1. U. Anand et al., Genes Dis. **10**, 1367 (2022).
2. C.Y. Zhao et al., Molecules. **23**, 826 (2018).
3. C.M. Tilsed et al., Front. Oncol. **12**, 960317 (2022)
4. Z. Cheng et al., J. Hematol. Oncol. **14**, 85 (2021)
5. H. Wang et al., J. Nanobiotechnol. **19**, 322 (2021)
6. X. Bai et al., Micromachines **13**, 1632 (2022)
7. S. Adepu, S. Ramakrishna, Molecules **26**, 5905 (2021)
8. M.T. Manzari et al., Nat. Rev. Mater. **6**, 351 (2021)
9. C. Carvalho et al., Curr. Med. Chem. **16**, 3267 (2009)
10. O. Tacar, P. Sriamornsak, C.R. Dass, J. Pharm. Pharmacol. **65**, 157 (2013)
11. M. Kciuk et al., Cells **12**, 659 (2023)
12. A.M. Meredith, C.R. Dass, J. Pharm. Pharmacol. **68**, 729 (2016)
13. A. Fukuda et al., PLoS ONE **12**, e0185654 (2017)
14. J. Lin et al., PLoS ONE **7**, e49277 (2012)
15. B. Zhu, H. Zhang, L. Yu, Biomed. Pharmacother. **86**, 547 (2017)
16. K. Aloss, P. Hamar, Pharmaceutics **15**, 893 (2023)
17. E.B. Lages et al., Biomed. Pharmacother. **144**, 112373 (2021)
18. D. Wang, X. Zhang, B. Xu, Front. Bioeng. Biotechnol. **9**, 781982 (2021)
19. Z.J. Chen et al., Nano Lett. **20**, 4177 (2020)
20. M.J. Mitchell et al., Nat. Rev. Drug Discov. **20**, 101 (2021)
21. J.K. Patra et al., J. Nanobiotechnol. **16**, 71 (2018)
22. C. Gonçalves, P. Pereira, M. Gama, Materials **3**, 1420 (2010)
23. M.J. Nirmala et al., RSC Adv. **13**, 8606 (2023)
24. S. Senapati et al., Signal Transduct. Target. Ther. **3**, 7 (2018)
25. A.M. Vargason, A.C. Anselmo, S. Mitragotri, Nat. Biomed. Eng **5**, 951 (2021)
26. J. Hwang et al., Macromol. Res. **27**, 657 (2019)
27. Y. Lu et al., Nat. Biomed. Eng **2**, 318 (2018)
28. A.K. Sood, M. Aggarwal, J. Chem. Sci. **130**, 1 (2018)
29. F. Palazzesi, M. Calvaresi, F. Zerbetto, Soft Matter **7**, 9148 (2011)
30. J. Gao, W. Ge, J. Li, Sci. China, Ser. B: Chem. **48**, 470 (2005)
31. M. Kang et al., J. Ind. Eng. Chem. **80**, 239 (2019)
32. B.F. Soeriawidjaja et al., Mol. Cryst. Liquid Cryst. **687**, 53 (2019)
33. L. Oktavia et al., J. Ind. Eng. Chem. **73**, 87 (2019)
34. Y. Xie et al., Front. Oncol. **13**, 1027254 (2023)
35. S.H. Park et al., Adv. Sci. **9**, e2200872 (2022)

36. Y. Xie et al., Front. Oncol. **13**, 1027254 (2023)
37. J. Hwang et al., J. Nanobiotechnol. **20**, 245 (2022)
38. J.S. Park et al., Macromol. Res. **30**, 811 (2022)
39. P. Nakhaei et al., Front. Bioeng. Biotechnol. **9**, 705886 (2021)
40. M.K. Lee, Pharmaceutics **12**, 264 (2020)
41. E. Christidi, L.R. Brunham, Cell Death Discov. **12**, 339 (2021)
42. S. Bien et al., Biochem. Pharmacol. **80**, 1466 (2010)

Publisher's Note Springer Nature remains neutral with regard to jurisdictional claims in published maps and institutional affiliations.

Authors and Affiliations

Juyoung Hwang[1,2,3] · Min-Hee Jo[3] · Chen Li[4] · Sun Joo Park[3] · Minseok Kwak[1,2,3,5]

✉ Minseok Kwak
mkwak@pukyong.ac.kr

[1] Industry 4.0 Convergence Bionics Engineering, Pukyong National University, Busan, Republic of Korea

[2] Smart Gym-Based Translational Research Center for Active Senior's Healthcare, Pukyong National University, Busan, Republic of Korea

[3] Department of Chemistry, Pukyong National University, 45 Yongso-Ro, Nam-Gu, Busan 48513, Republic of Korea

[4] School of Materials Science and Engineering, Guangdong Province, Dongguan University of Technology, Songshan Lake, No.1, Daxue Road, Dongguan, People's Republic of China

[5] Department of Chemistry and Industry 4.0 Convergence Bionics Engineering, Pukyong National University, 45 Yongso-Ro, Nam-Gu, Busan 48513, Republic of Korea